Additional Figures for "A Comparison Study of Extreme Precipitation from Six Different Regional Climate Models via Spatial Hierarchical Modeling"

Erin M. Schliep, Daniel Cooley, Stephan R. Sain, and Jennifer A. Hoeting

This document contains color versions of the figures that appear in the paper as well as additional figures that were produced in preparing the aforementioned paper. The figures are:

Color versions of the figures in the paper.

1. qqPlot of results.
2. Posterior mean of the return level.
3. Standard deviation of return level.
4. Difference of return levels.
5. F-statistic plots for return levels and ξ.
6. Posterior mean of ξ.
7. Pointwise estimates of return levels and ξ.

Additional figures

8. Posterior mean map for μ.
9. Posterior mean map for σ.
10. Posterior mean map for ξ.
11. Posterior variance map for μ.
12. Posterior variance map for σ.
13. Posterior variance map for ξ.

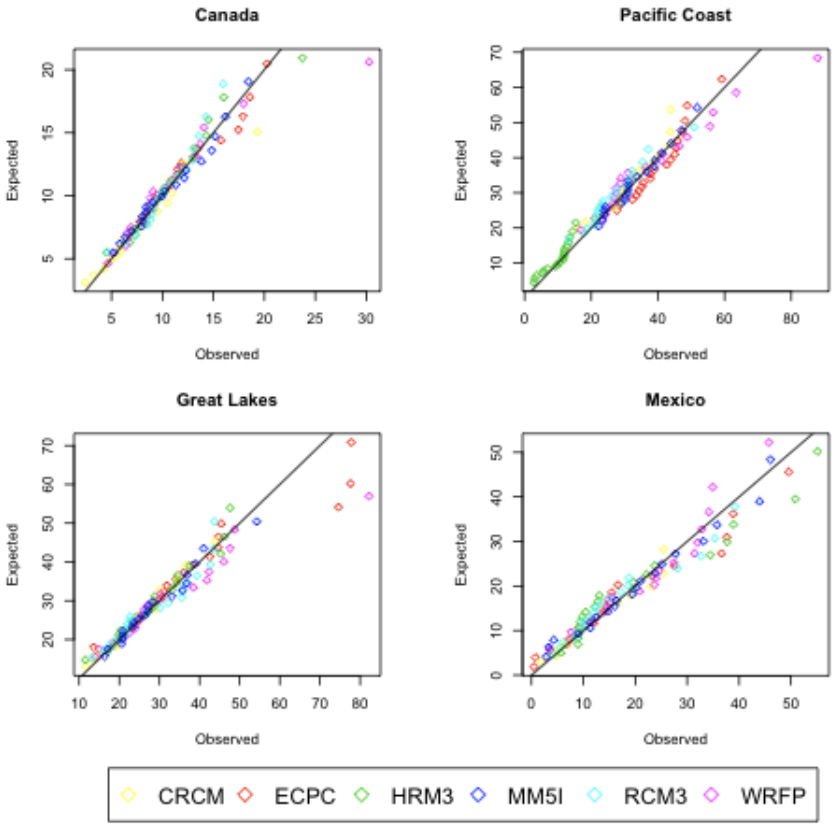

Figure 1: Quantile-quantile plots for four locations within our region. The values are given in mm/day and the scales vary based on the precipitation values at each location.

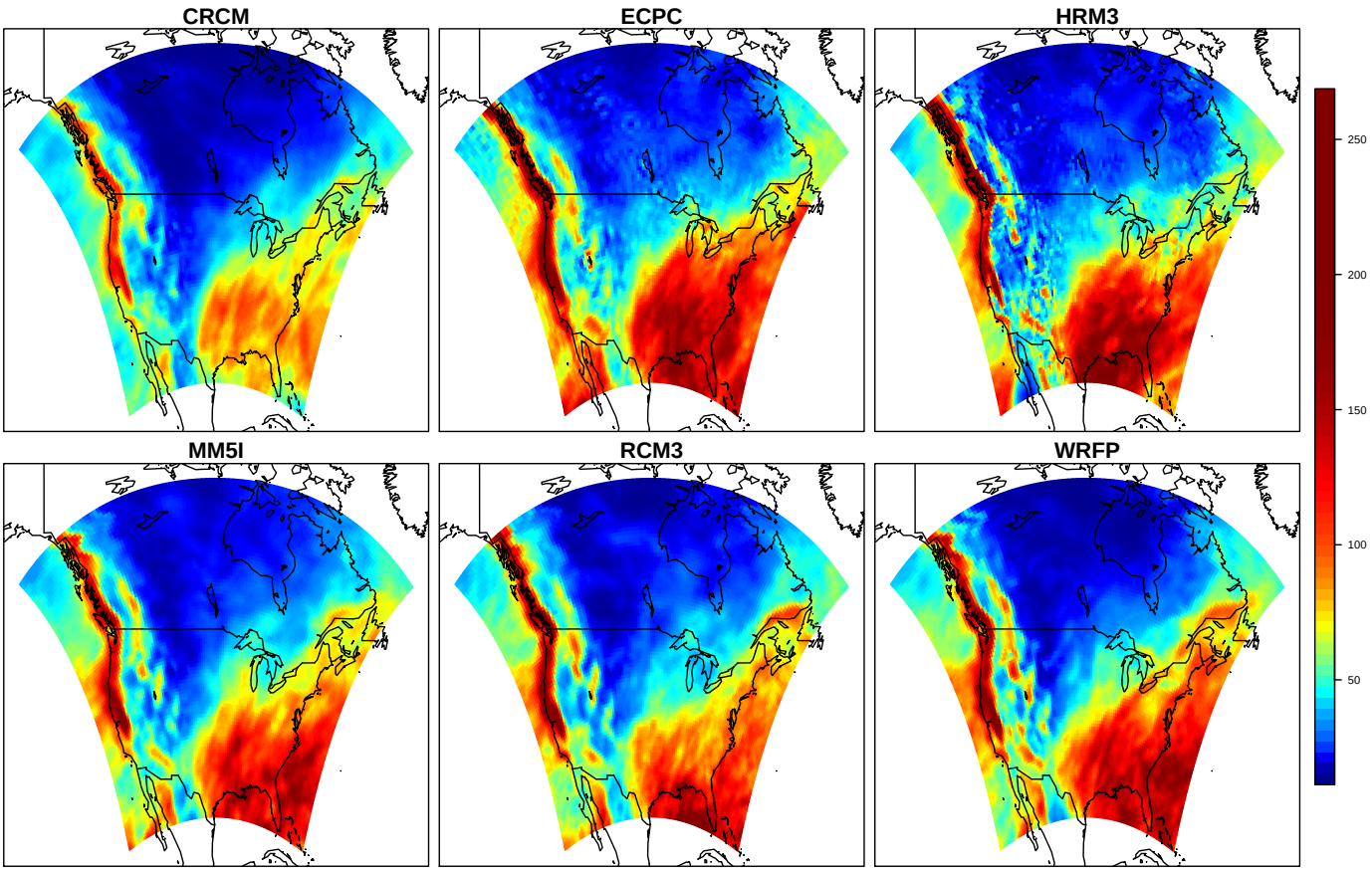

Figure 2: Mean of the posterior distribution of 100 year return levels for daily winter precipitation (in mm) for each of the six RCMs. All show a pattern of higher return levels for the Pacific Northwest and the Southeast United States and a much lower 100 year return level for central Canada. Precipitation is given in mm/day.

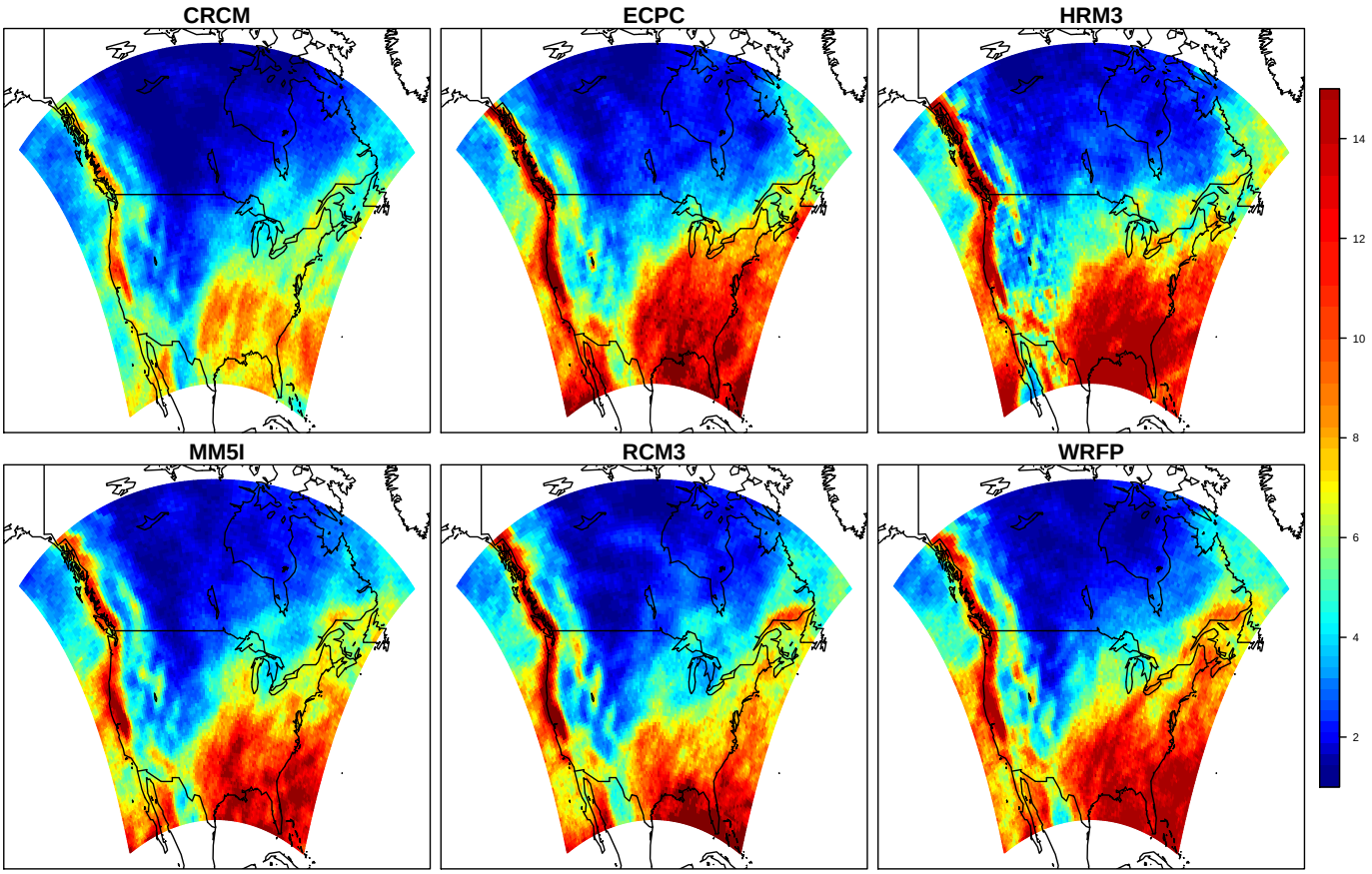

Figure 3: Standard deviations of the posterior distribution of 100 year return levels for daily winter precipitation for each of the six RCMs. Locations of high variation correspond to locations that show higher mean precipitations in Figure 2. Values were cut off at 15 to better contrast the lower values.

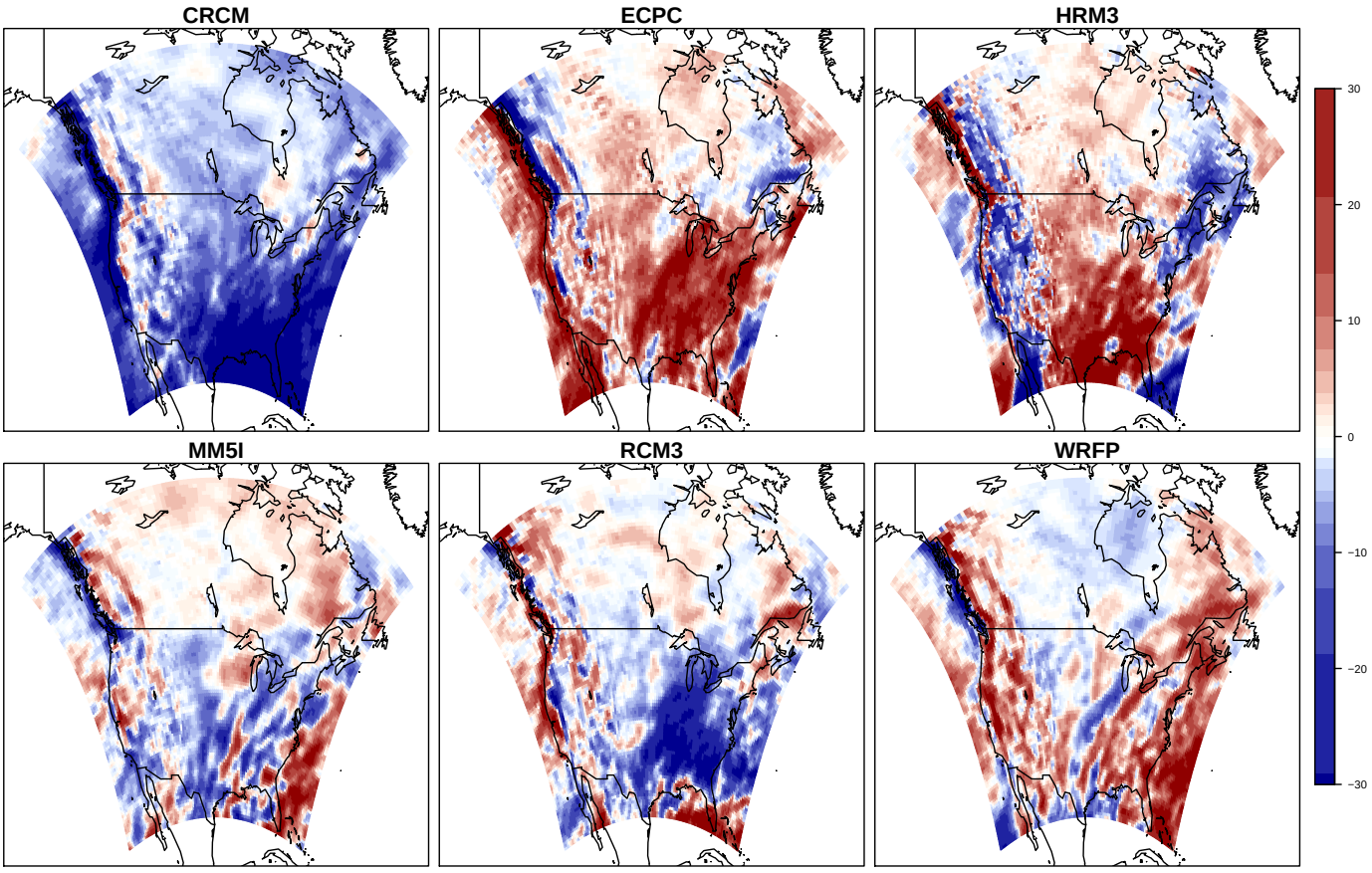

Figure 4: Difference between the posterior mean of 100 year return levels for each model and the overall posterior mean of return levels across models. Despite the similar patterns shown in Figure 2, this shows that there are considerable differences in the estimated return levels from model to model. The difference in values are given in mm/day. Values were cut off at -30 and 30 to better present the values near 0.

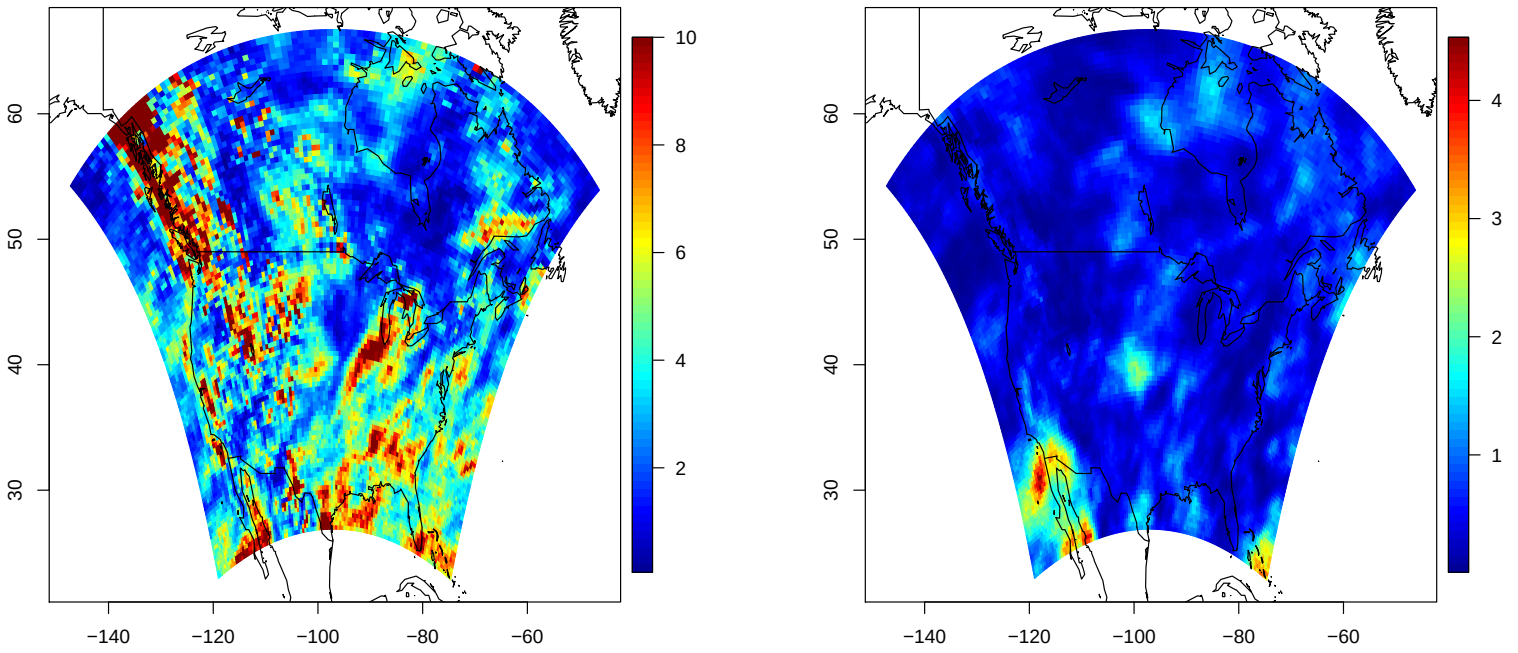

Figure 5: Left Panel: The pointwise F-statistic for the return level comparison, the between-model variance divided by the within-model variance. The nominal 95% quantile of the $F_{5,5995}$ is 2.22. As many locations show an F-statistic larger than this value, one can see that the differences found in Figure 4 appear to be significant, although performing an actual hypothesis test is complicated due to both multiple testing concerns and spatial dependence. Values were cut off at 10 so as to better contrast the lower values of the scale. Right panel: The pointwise F-statistic for the model-to-model comparison for ξ. Despite the differences seen in the point estimates in Figure 6, few areas show an F-statistic greater than the 95% quantile of 2.22 due to the considerable uncertainty associated with the estimation of ξ.

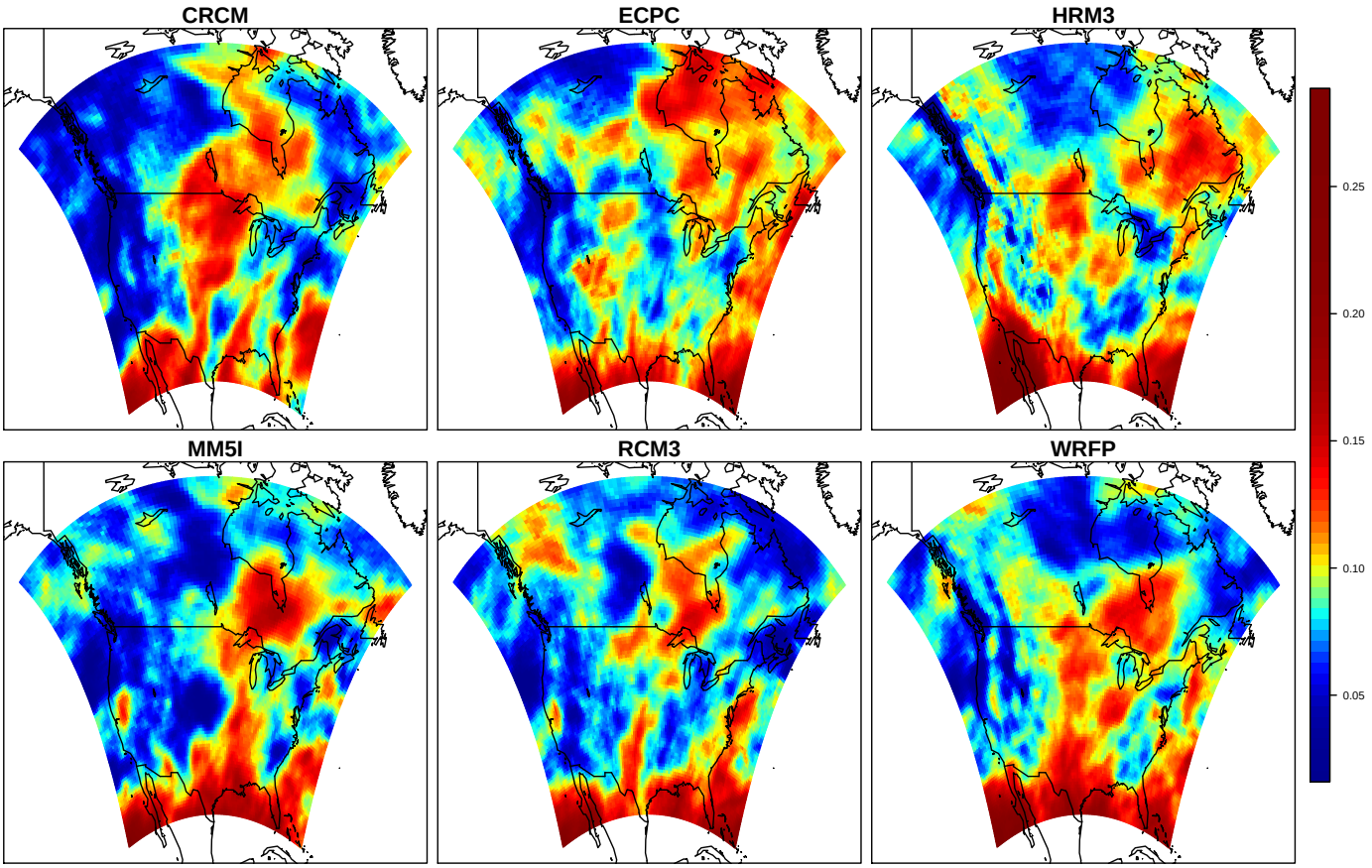

Figure 6: Mean of the posterior distribution for the extreme value index ξ. While there are some general similarities in the point estimates such as heavier tails in the center of the continent, there is considerable variability in the patterns of the point estimates from model to model.

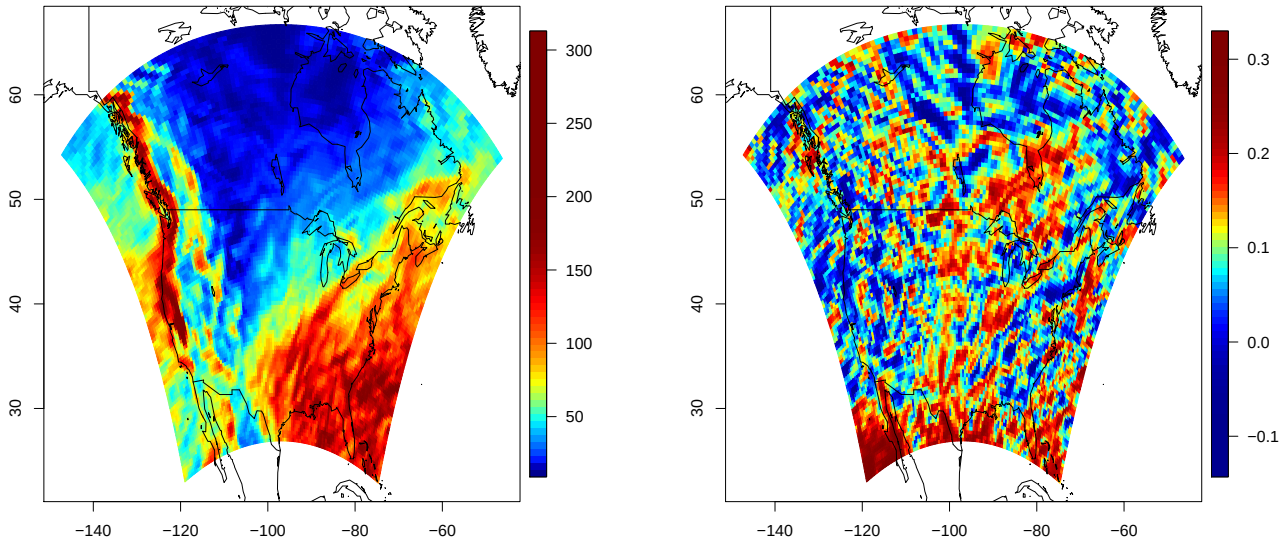

Figure 7: Left panel shows the estimated 100-year return level for the WRFP model as obtained via maximum likelihood estimates for μ, σ, ξ done via a point-by-point analysis. Right panel shows the estimated shape parameter ξ as obtained via penalized maximum likelihood using the Stedinger prior, also done via a point-by-point analysis. In addition to being less smooth, both show an increased range of values compared to Figures 2 and 6.

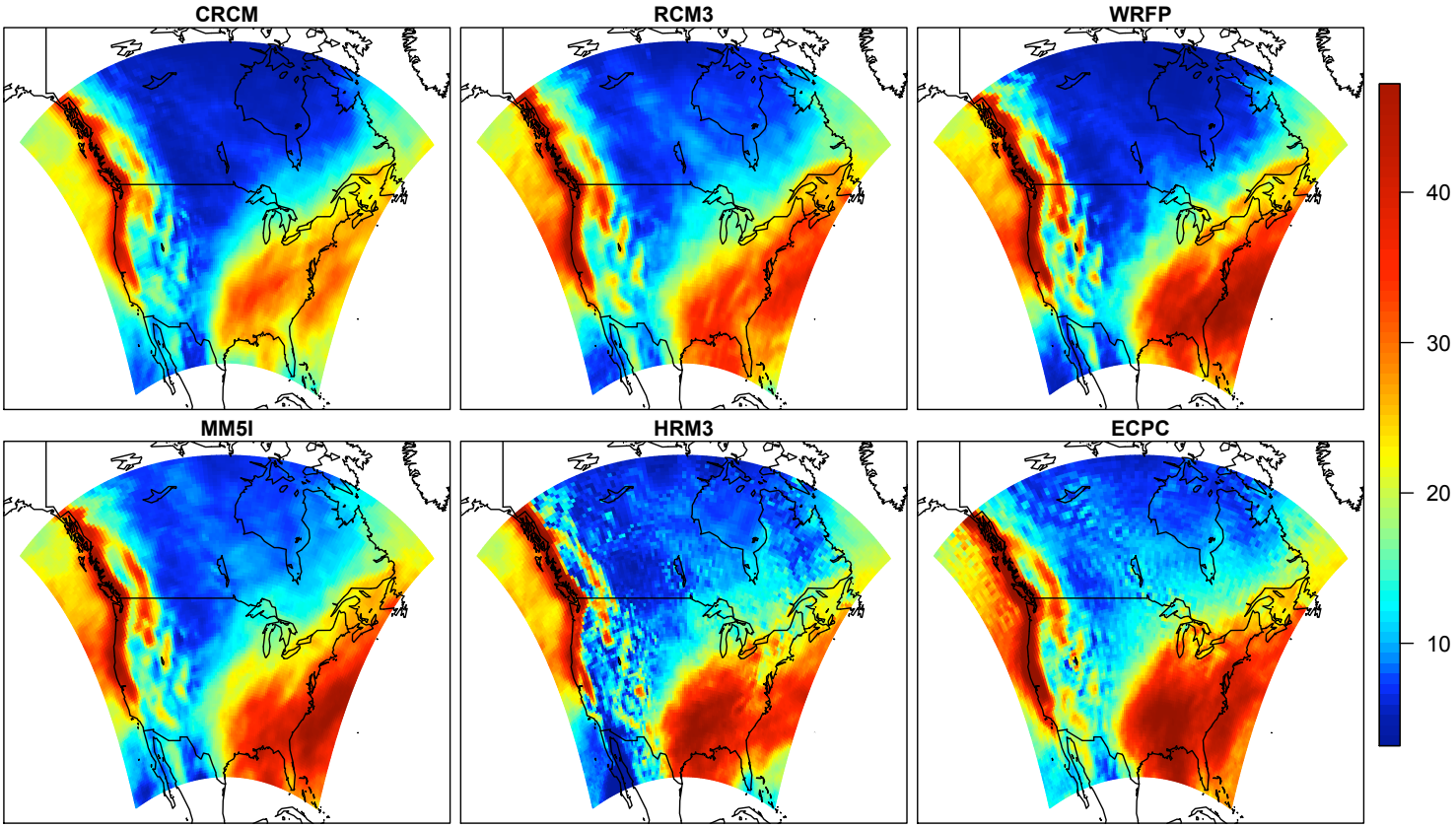

Figure 8: Posterior mean for μ parameter for the six RCMs

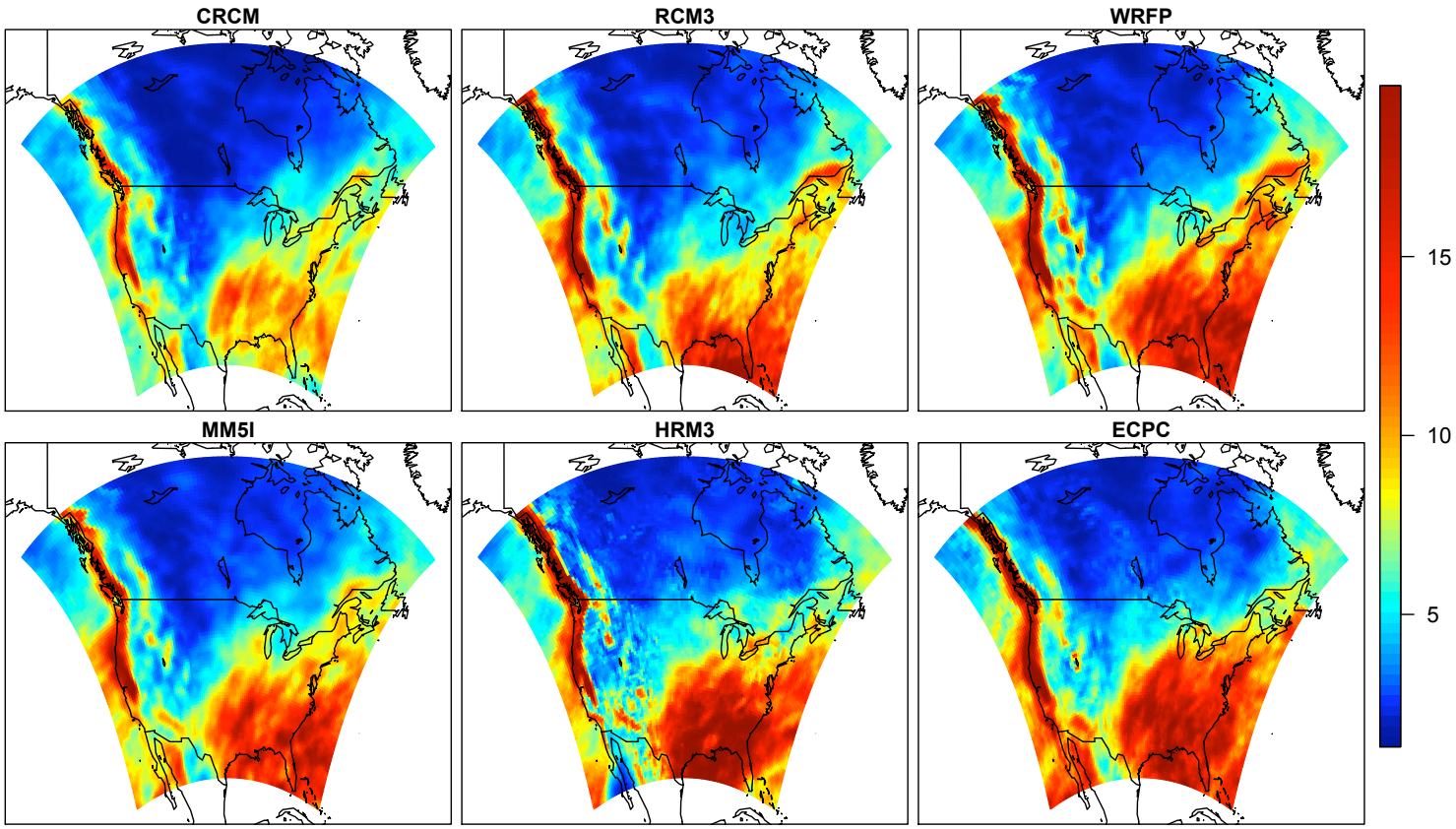

Figure 9: Posterior mean for σ parameter for the six RCMs

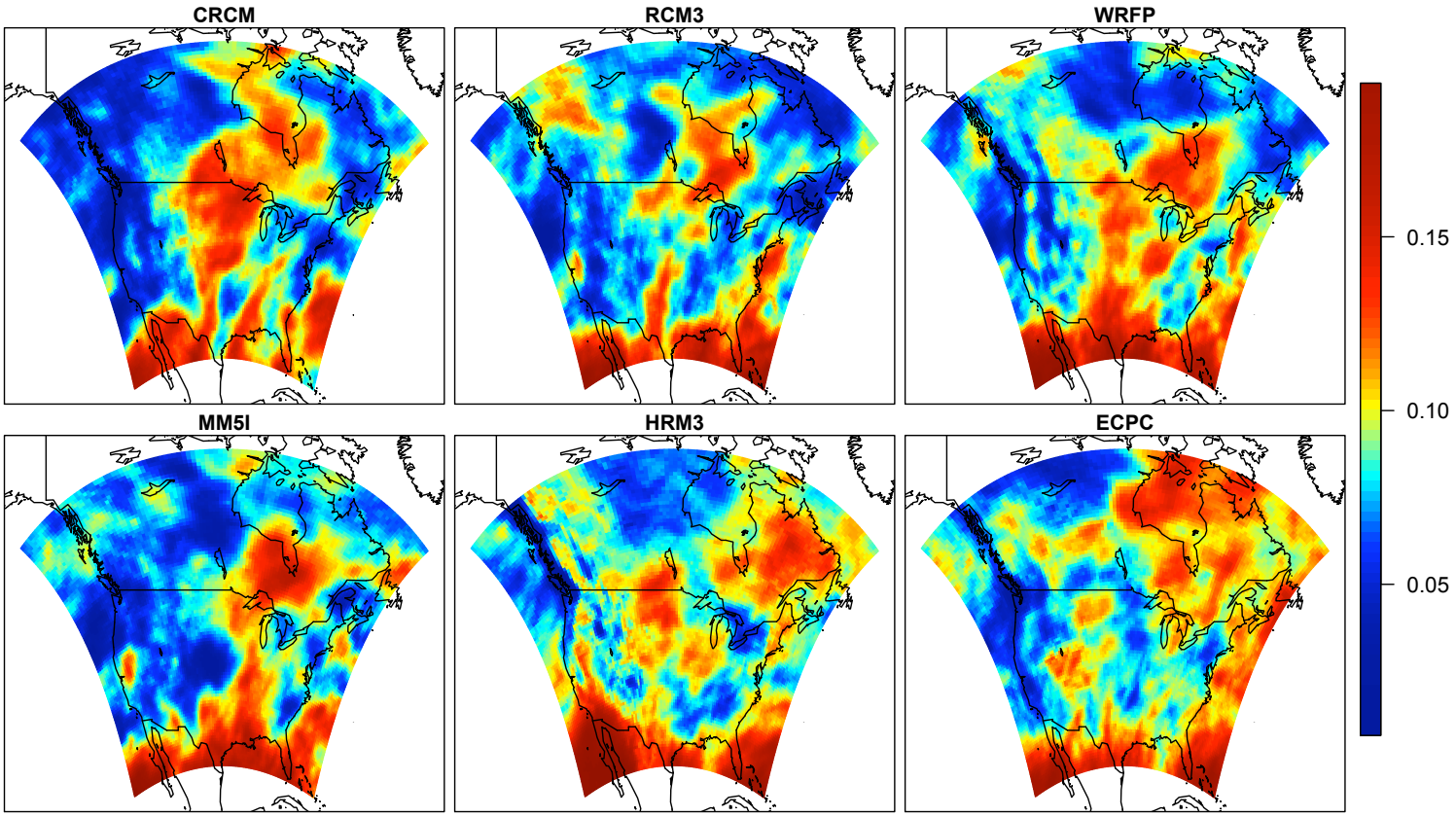

Figure 10: Posterior mean for ξ parameter for the six RCMs

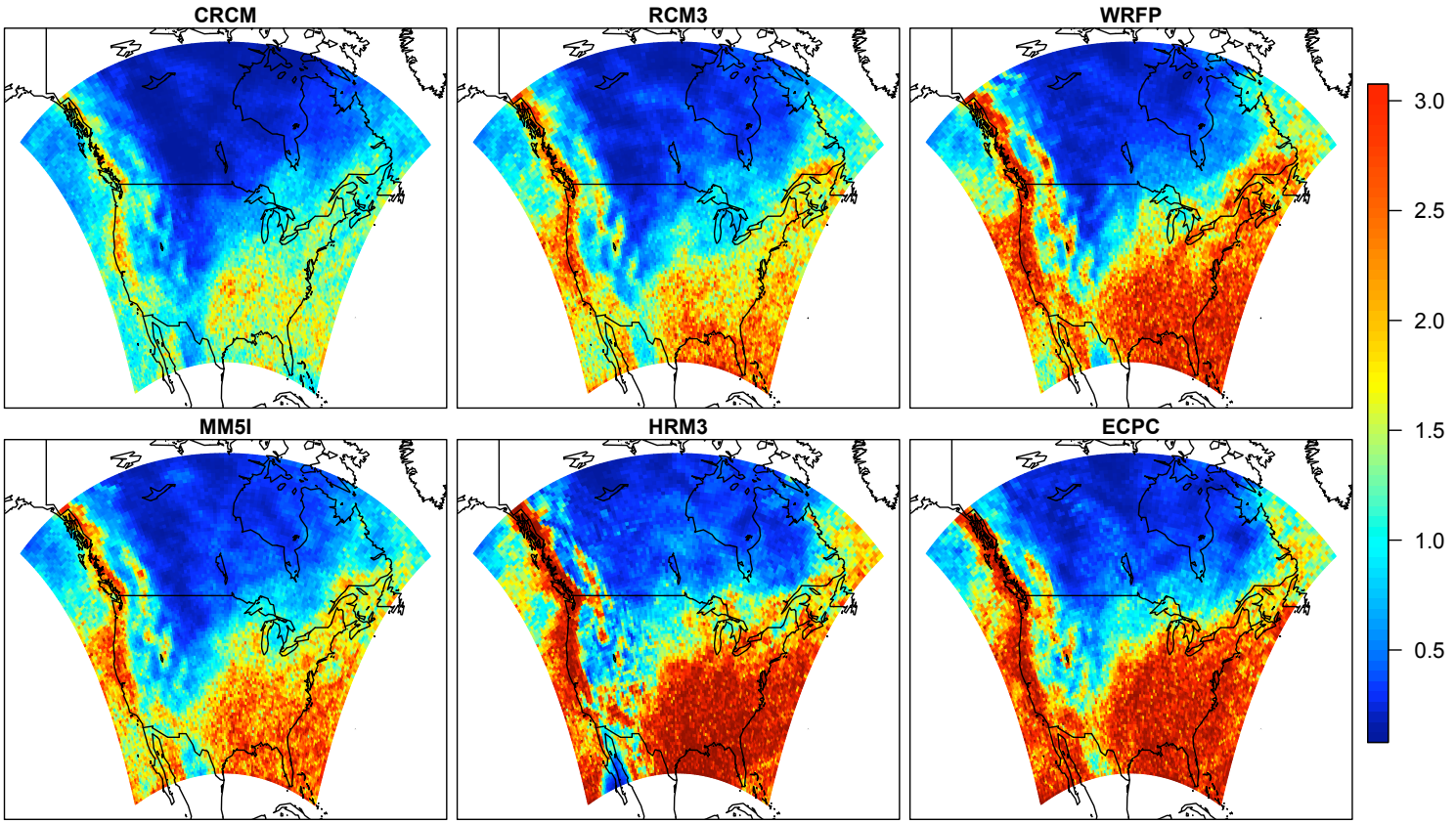

Figure 11: Posterior variance for μ parameter for the six RCMs

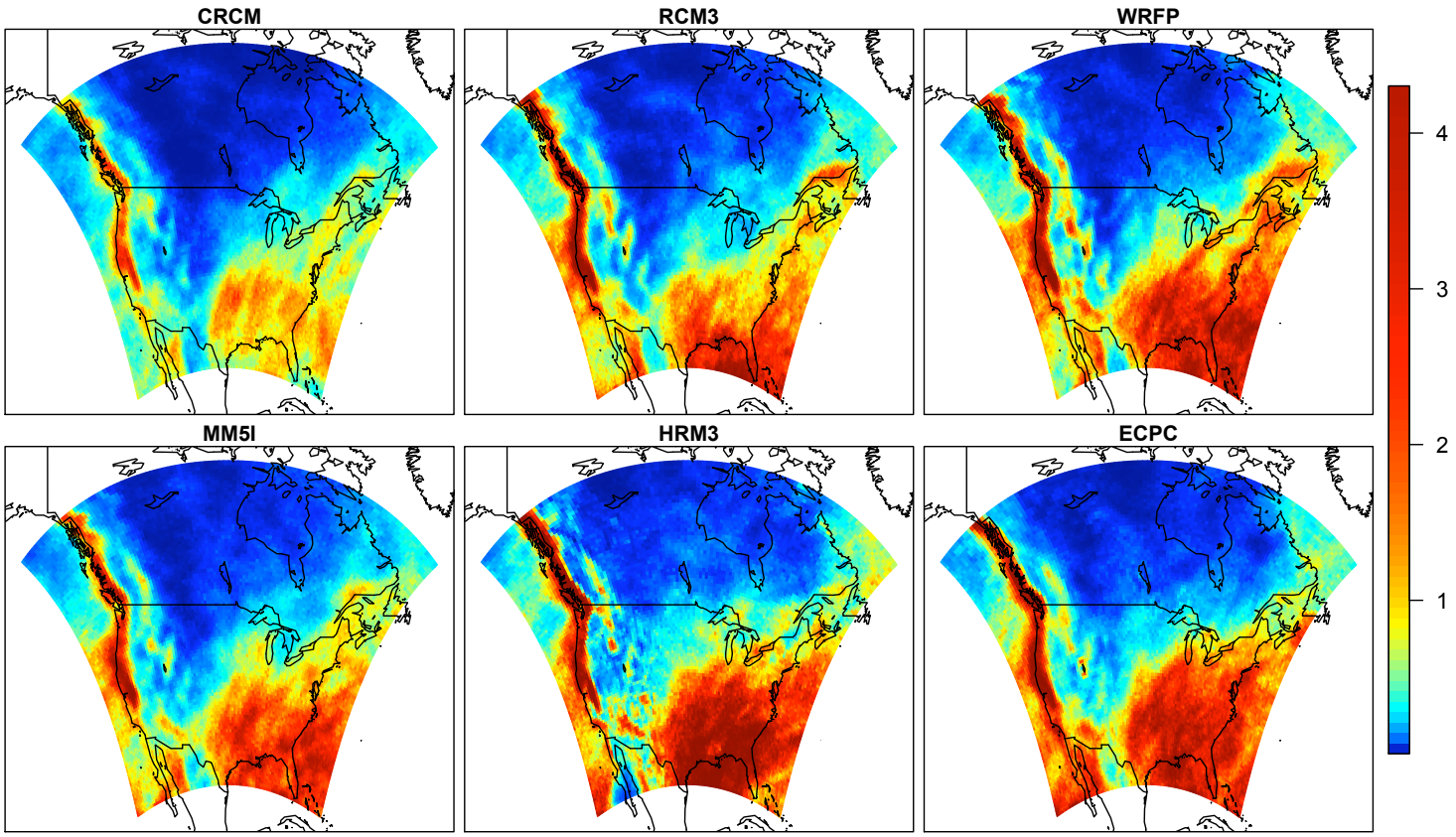

Figure 12: Posterior variance for σ parameter for the six RCMs

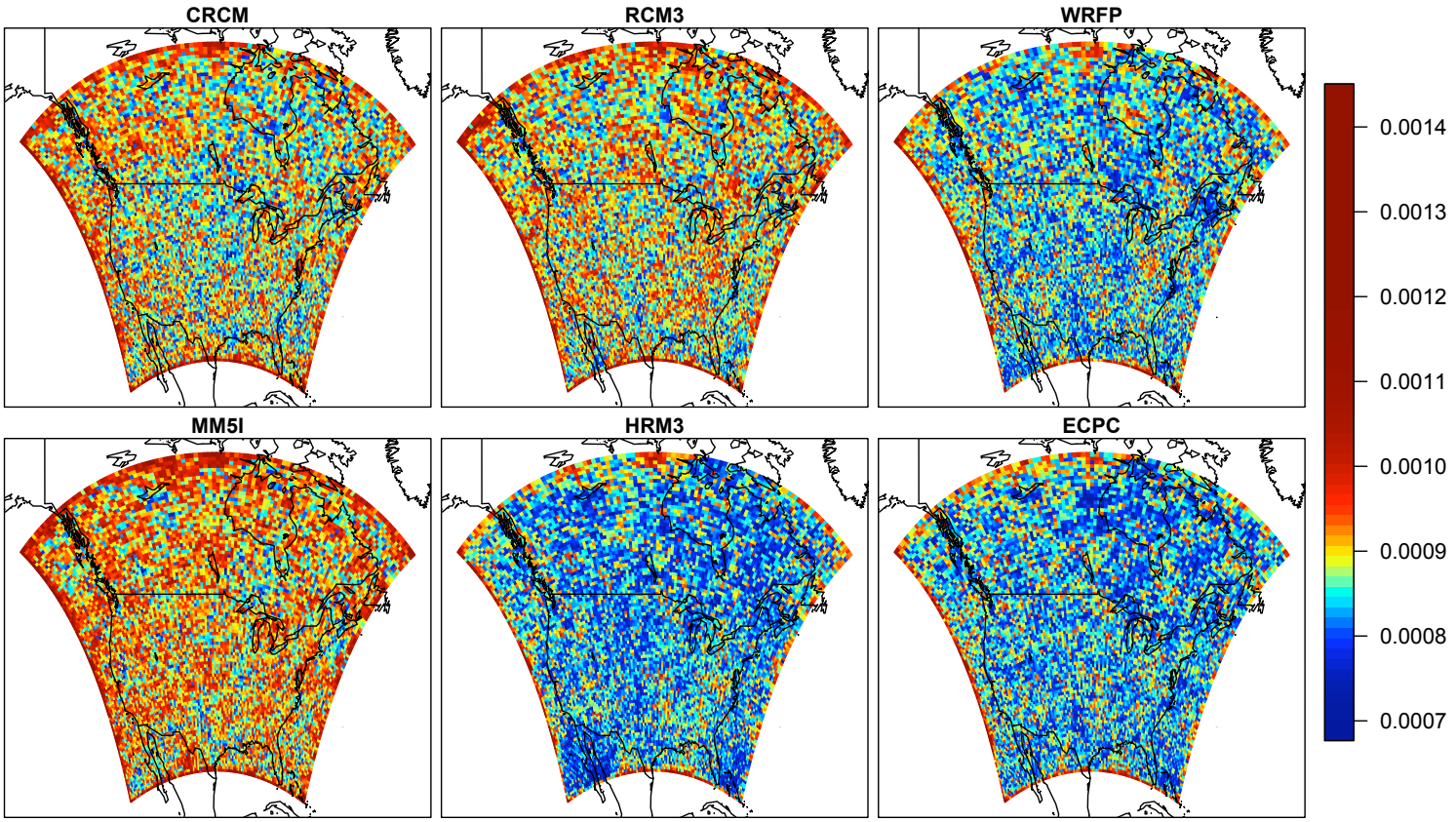

Figure 13: Posterior variance for ξ parameter for the six RCMs

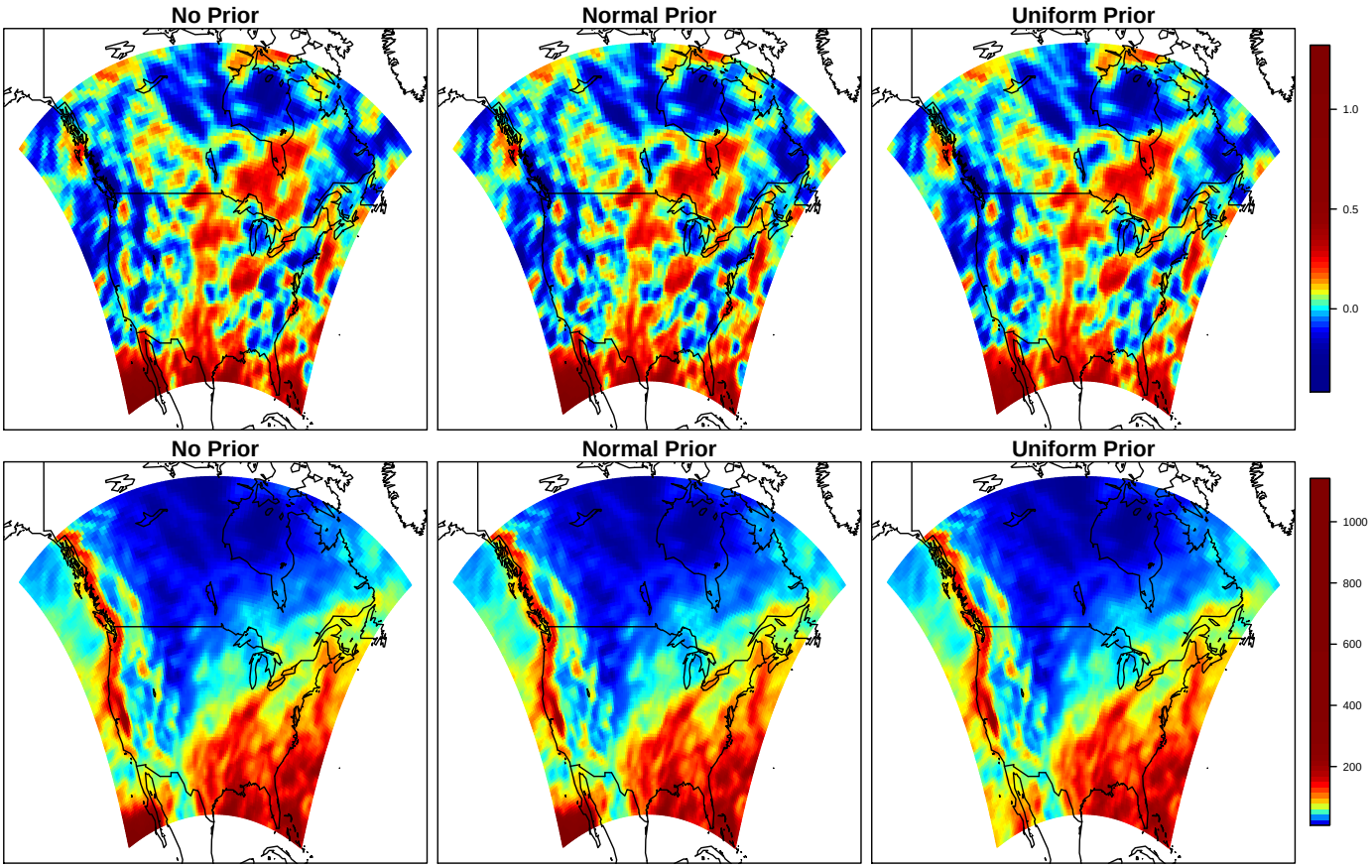

Figure 14: Sensitivity analysis to the penalty on the shape parameter. Maps show the mean of the posterior distribution for the shape parameter ξ and the return level (bottom) for three different penalties on the shape parameter.